International Journal of Engineering

Journal Homepage: www.ije.ir

Role of Praseodymium Addition in the Microstructure and Magnetic Properties of ZnCo Ferrite Nanopowders: Positive or Negative?

B. Shahbahrami[a], S. M. Rabiee[a*], R. Shidpoor[a], H. Salimi-Kenari[b]

[a] *Department of Materials Engineering, Babol Noshirvani University of Technology, Babol, Iran*
[b] *Faculty of Engineering & Technology, University of Mazandaran, Babolsar, Iran*

PAPER INFO

Paper history:
Received 19 September 2021
Received in revised form 08 October 2021
Accepted 10 October 2021

Keywords:
Cobalt Ferrite
Coprecipitation
Cation Distribution
Microstructure Properties
Magnetic Propertie

ABSTRACT

In order to investigate the effect of praseodymium (Pr) addition on the microstructure and magnetic properties of cobalt-zinc ferrite nanoparticles (NPs), different values of Pr element (x=0.2, 0.4 and 0.6) were added to the initial composition ($Co_{0.6}Zn_{0.4}Fe_{2-x}Pr_xO_4$) in the co-precipitation method, and the prepared precipitates calcined at 750 °C for 2 h. The synthesized powders were characterized by X-ray diffraction (XRD), field emission electron microscopy (FESEM), Fourier transform infrared spectroscopy (FTIR), and vibrating sample magnetometer (VSM). XRD pattern revealed the formation of a secondary phase of Pr-Fe oxide in addition to the ZnCo ferrite phase in the samples. FESEM images showed changes in the morphology and size of the particles by adding Pr to the composition. For specimen with x=0.2, the homogeneous spherical like particles with the size about less than 60 nm was formed. Whereas, for composition containing x=0.6 of Pr, a non-uniform powder with plate like particles was obtained and NPs had a thickness of approximately less than 30 nm. VSM analysis indicated that by increasing the element Pr to the cobalt-zinc ferrite composition, especially for values higher than x=0.2, the powder become a completely non-magnetic material.

***doi**: 10.5829/ije.2022.35.01a.02*

NOMENCLATURE

XRD	X-ray diffraction	H_C	Coercive force
FESEM	Field emission scanning electron microscopy	n_B	Bohr magneton
VSM	Vibrating sample magnetometer	Mr	Remanence magnetization
M_S	Saturation magnetization	a	Lattice parameter (Å)
K	Anisotropic constant	D	Crystallite size (Å)

1. INTRODUCTION

The magnetic properties of ferrites with spinel structure and their application depend on the composition and distribution of the cations at the tetrahedral (A) and octahedral (B) spaces [1-4]. Accordingly, many researchers have replaced various elements in the spinel structure and have studied changes in magnetic properties such as the saturation magnetism (Ms), coercive force (Hc), anisotropy constant (K), remanence magnetization (M_r), and the magnetic moment (n_B). Cobalt ferrite is an interesting material due to its high magnetic permeability, high coercive force, good saturation magnetization (Ms) and usability in a wide range of applications such as telecommunications and medicine [2, 5]. Therefore, research is underway to study the effect of element substitution on cobalt ferrite materials. For example, Topkaya et al. [6] synthesized cobalt ferrite nanoparticles (NPs) substituted with zinc element ($Zn_xCo_{1-x}Fe_2O_4$) by hydrothermal method. The highest M_S of 76.5 emu/g reported for ferrite containing x=0.2. In addition, they stated that Zn^{2+} ion is located in A site, forcing Fe^{3+} ions to move from the A position to the B space. Dalal et al. [7] also synthesized $Ni_{0.4}Zn_{0.4}Co_{0.2}Fe_2O_4$ NPs by co-precipitation method and obtained crystallites with a size of about 34.7 nm and

*Corresponding Author Institutional Email: rabiee@nit.ac.ir (S. M. Rabiee)

Please cite this article as: B. Shahbahrami, S. M. Rabiee, R. Shidpoor, H. Salimi-Kenari, Role of Praseodymium Addition in the Microstructure and Magnetic Properties of ZnCo Ferrite Nanopowders: Positive or Negative?, ***International Journal of Engineering, Transactions A: Basics*** Vol. 35, No. 01, (2022) 14-20

high magnetization (84 emu/g) at room temperature. Ramakrishna et al. [8] synthesized $Co_{0.5}Zn_{0.37}Cu_{0.13}Fe_2O_4$ NPs with crystallite diameters 82.41 nm via sol-gel method. They reported Ms, H_c, K and n_B of the NPs equal to 50.35 emu/g, 198.9 Oe, 1.7 x 10^4 erg/Oe and 2.9 μB, respectively.

In another study by Naik and, Salker [9], the effect of adding Dy and Gd elements on magnetic properties of the cobalt ferrite NPs at room temperature (300 K) and very low temperature (5 K) investigated. With analysis of their results, it was found that firstly, lowering the temperature increased the saturation magnetization and the coercive field. The reason for this is activation of the magnetic moments of Dy and Gd ions at temperatures below 40 K. By substituting Dy^{3+} and Gd^{3+}ions instead of Fe^{3+}, the magnetic moment of the B sties, saturation magnetization and the coercive field increases. In addition, it observed that the amount of M_S in Dy-doped cobalt ferrite NPs (70.29 emu/g) is higher than that of Gd-doped specimen (60.85 emu/g) at room temperature. The higher magnetic moment in Dy ions than Gd ions mentioned for this difference.

In the work of Xavier et al. [10], the effect of samarium on the structural and magnetic properties of cobalt ferrite NPs ($CoFe_{2-x}Sm_xO_4$) investigated. They stated that with increasing Sm^{3+} concentration to x=0.25, the crystallites size increases from 11.26 to 16.53 nm, which is due to the higher ionic radius of the samarium than the iron element. For this reason, the coercive force reduced from 1372.2 Oe to 814.73 Oe, which is due to the easier movement of magnetic domains.

Alves et al. [11] studied the effect of adding Y^{3+} ions on the structural and magnetic properties of cobalt ferrite NPs ($CoY_xFe_{2-x}O_4$). By increasing the Y^{3+} ion values to 0.04, the grain size of the sample decreased from 35.32 to 16.05 nm. The saturation magnetization also decreased from 69 emu/g to 33 emu/g, while the coercive force increased from 1100 Oe to 1900 Oe.

In order to control particle size at high calcination temperatures and improve magnetic properties, Panda et al. [12] doped rare earth elements Pr or Gd in cobalt ferrite compositions and calcined them at different temperatures. They stated that the single-domain size of the pure cobalt ferrite materials is 70 nm. On the other hand, with increasing the calcination temperature to more than 500 ° C, the size of the crystallites significantly increases, so the presence of rare earth elements in the ferrite structure prevents their growth. The crystallite sizes of the samples synthesized by them for the compounds $CoGd_{0.1}Fe_{1.9}O_4$, $CoPr_{0.1}Fe_{1.9}O_4$, $CoGd_{0.2}Fe_{1.8}O_4$ and $CoPr_{0.2}Fe_{1.8}O_4$ at 900 °C were equal to 41.4, 33.2, 65.6 and 57.5 nm, respectively, while for pure cobalt ferrite it was 87.5 nm.

We know that the particle size plays a role in the relaxation time according to Equation (1), and the rapid switching of magnetic behavior occurs with smaller particles [13-15].

$$\tau_N = \tau_0 e^{(KV/k_BT)} \quad (1)$$

where τ_N is the Neel relaxation time, τ_0 is the exponential parameter ($\tau_0=10^{-9}$-10^{-3} s^{-1}), K is the anisotropy constant, V is the volume of NPs, K_B is Boltzmann constant, and T is the temperature (K_BT is thermal energy).

n the other hand, the amount of magnetic moment theoretically depends on the difference in magnetic moment between the tetrahedral and octahedral spaces according to Equation (2) [6, 16, 17]. Therefore, with the introduce of an even non-magnetic element into the ferrite composition and its replacement instead of one of the elements in A or B spaces, the initial order of ions is disturbed and may lead to a difference in the magnetic moment of the material.

$$nB(cal.) = MB(x) - MA(x) \quad (2)$$

Therefore, in the present work, the element praseodymium is added to the zinc cobalt ferrite composition and its effect on the microstructure and magnetic properties is studied, which has not been investigated by others. In this composition, by doping Zn in cobalt ferrite structure, it is expected to increase the crystallite sizes and saturation magnetization, and reduce the coercive force. By adding Pr to the composition, this element is located in the octahedral spaces instead of iron element and acts like non-magnetic atoms at room temperature. However, it is used for this research for two reasons; first, due to the unpaired electrons in the *4f* layer, it has a single ion anisotropy in the crystal lattice, which may be useful. Second, by changing the particle size and surface effects due to inhibiting the growth of particles and the crystallite diameters beyond the range of single-domain size (70 nm) may improve the microstructure and magnetic properties.

2. EXPERIMENTAL

Nanocrystalline powders ($Co_{0.6}Zn_{0.4}Fe_{2-x}Pr_xO_4$, x=0.2, 0.4 and 0.6) were prepared by co-precipitation method using raw materials of iron nitrate ($Fe(NO_3)_3.9H_2O$) (Merck), cobalt nitrate ($Co(NO_3)_2.6H_2O$) (Merck), zinc nitrate ($Zn(NO_3)_2.4H_2O$) (Merck), and praseodymium nitrate ($Pr(NO_3)_3.6H_2O$) (Merck). Using deionized water (DI), 0.5 M solutions were prepared from each of the starting materials. The solutions were stirred for 10 m on a magnetic stirrer (50 °C, 400 rpm). These solutions were mixed together. The pH of the mixture was raised to 11 using NaOH (Merck) and stirred again (5 h, 80 °C, 700 rpm). The resulting precipitates were dried (110 °C, 24 h), then calcinated (750 °C, 2 h). The phase formation and strain created in the particles were studied by XRD (D8 ADVANCE, BRUKER, Germany) technique. FESEM (Mira 3-XMU) was used to investigate the

morphology and size of the particles, and FTIR (Shimadzu Co., Japan) was performed in order to evaluate the chemical bonds in the synthesized specimens. Also magnetic properties of the prepared samples were identified using VSM (Danesh Pajooh Co., Iran) analysis. From now on, specimens with different Pr values are introduced as Pr0 to Pr6 according to Pr content (x).

3. RESULTS AND DISCUSSION

The XRD results of the synthesized samples at 750 °C for 2 h are shown in Figure 1. It should be noted that in order to compare and evaluate the effect of adding Pr to the composition, XRD analysis of the Pr free sample is also provided.

In the sample without Pr (Pr0) (Figure 1-a), the appearance of planes (220), (311), (222), (400), (422), (511), (440), (622) and (533) according to JCPDS card 00-022-1086 confirms the formation of single-phase ZnCo ferrite with cubic spinel structure. By adding Pr to the composition equal to x= 0.2 (Pr2) (Figure 1-b), it can be seen that in addition to the previously appeared peaks, other peaks are formed at other angles, which according to JCPDS 01-074-1472 belong to the new phase of Pr-Fe oxide ($PrFeO_3$). As the amount of praseodymium increased, the intensity of the new phase peaks also increased, and the height of the initial spectra in the Pr-free sample was significantly reduced, and even many peaks were removed (Figure 1-d). In fact, the predominant phase in these specimens is $PrFeO_3$. This means that contrary to expectations, with the presence of praseodymium in the reaction system, no solid solution of CoZnPr ferrite is formed. This result contradicts the findings reported by Panda et al. [12] that synthesized cobalt ferrite substituted with Pr^{3+} ($CoFe_{1-x}Pr_xO_4$) using citrate raw materials by sol-gel method and obtained $CoPr_{0.1}Fe_{1.9}O_4$ and $CoPr_{0.2}Fe_{1.8}O_4$. This is probably due to the higher ionic radius of praseodymium (1.13 Å) than iron (0.67 Å) [16], which makes it difficult to place as a substituent or interstitial element within the structure.

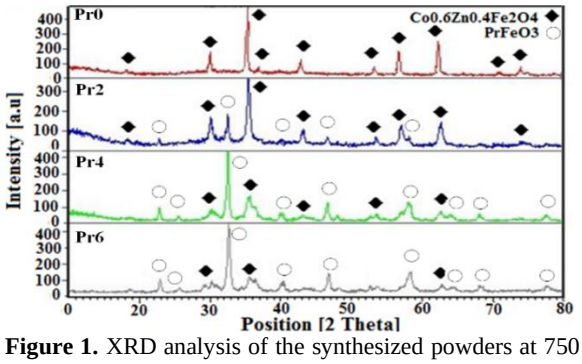

Figure 1. XRD analysis of the synthesized powders at 750 °C for 2 h

The Bertaut method was used to calculate the amount of phases which is based on the intensity of the scattered peaks and is summarized in Table 1. It is observed that in the composition with x=0.2, equivalent to 30.94 wt. % of the new phase ($PrFeO_3$) is formed. This amount increased to 84.23 wt. % in the composition containing x=0.6, which means a reduction of the initial phase ($Co_{0.6}Zn_{0.4}Fe_2O_4$) to 15.77 wt.% in the powder.

The crystallite diameters and the strain created inside the crystalline particles were obtained by Williamson-Hall equation [18-20] as follows:

$$B.\cos(\theta) = (0.9.\lambda / D) + 4\,\varepsilon \sin(\theta) \quad (3)$$

where, D is the grain size (Å), λ is the wavelength of $Cu_{k\alpha}$ (1.54056 Å), B is the broadening line at half the peak height (rad.), ε is the lattice strain, and θ is the Bragg angle of the scattered peak.

The results of the Williamson-Hall equation for the synthesized samples are summarized in Table 2.

It is observed that the sample without Pr has a crystallite diameter of 47.81 nm and a compressive strain equal to 10^{-4}. When praseodymium introduce to the composition, the strain created in the ZnCo ferrite is tensile type and this strain increases with increasing amount of Pr element. Due to the increase in tensile strain, the diameter of its crystallites also decreases further. On the other hand, the strain created in the Pr-Fe oxide phase is compressive type. As a result, the diameter of its crystallites increases. The diagram of changes in the crystallite diameters in terms of the Pr value for each of the phases is given in Figure 2.

The lattice parameter of the synthesized powders was also obtained using extrapolate function $\cos^2\theta/\sin\theta$ [21] (Table 3).

The chemical bonds in the synthesized specimens are shown in Figure 3. The vibrational modes appeared at 450 cm^{-1} and 590 cm^{-1} are related to M-O bonds in the B and A spaces of the ferrite phase, respectively. The stretching modes at 1650 cm^{-1} and 3450 cm^{-1} are belong to hydroxyl groups which can help to establish the surface bonds of the particles. The frequency band around 2350 cm^{-1} is attributed to C-H bond. Weak bands in the range 1250-1700 cm^{-1} are also related to –C=C– bonds [22-25].

TABLE 1. The relative intensity of the spectra appearing (I_{100}) and the amount of phases formed in the synthesized powders

Sample	Pr0	Pr2	Pr4	Pr6
Relative intensity (I_{100}) of ($Co_{0.6}Zn_{0.4}Fe_2O_4$)	100	100	31.83	18.72
Relative intensity (I_{100}) of ($PrFeO_3$)	0	44.81	100	100
$I_{PrFeO3}/I_{Co0.6Zn0.4Fe2O4}$	0	0.45	3.14	5.34
$PrFeO_3$ (Wt. %)	0	30.94	75.86	84.23
$Co_{0.6}Zn_{0.4}Fe_2O_4$ (Wt. %)	100	69.06	24.14	15.77

TABLE 2. Strain and crystallite size of the synthesized nanopowders at 750 °C for 2 h

Sample	Pr0	Pr2		Pr4		Pr6	
		Zn- Co Ferrite	Pr –Fe Oxide	Zn- Co Ferrite	Pr –Fe Oxide	Zn- Co Ferrite	Pr –Fe Oxide
$2\Theta_1$ (°)	35.37	35.48	32.53	35.48	32.56	35.78	32.68
$2\Theta_2$ (°)	62.46	30.15	46.66	62.69	46.68	30.23	46.81
$2\Theta_3$ (°)	56.88	62.67	58.23	30.22	58.27	62.90	58.34
$2\Theta_4$ (°)	30.04	57.10	22.79	57.05	22.86	58.34	22.95
B_1 (°)	0.26	0.45	0.28	0.93	0.34	0.70	0.41
B_2 (°)	0.32	0.46	0.33	0.61	0.37	0.62	0.42
B_3 (°)	0.34	0.51	0.35	0.64	0.64	0.31	0.64
B_4 (°)	0.22	0.48	0.19	0.46	0.31	0.64	0.38
ε	10^{-4}	$-2*10^{-4}$	$16.5*10^{-4}$	$-6.6*10^{-4}$	$35*10^{-4}$	$-45*10^{-4}$	$24*10^{-4}$
D (nm)	47.81	17.55	57.77	9.29	72.97	8.56	33.01

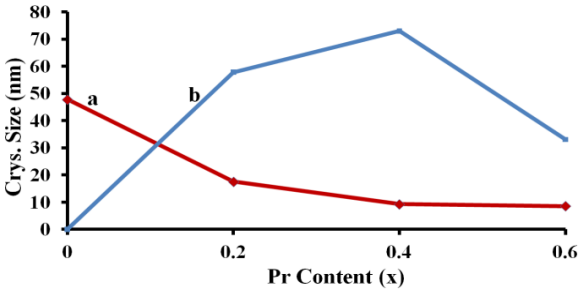

Figure 2. The crystallite diameter of the synthesized samples as a function of Pr value; (a) Crystallite diameter of ZnCo ferrite, and (b) Crystallite diameter of Pr-Fe oxide

The FESEM images of the synthesized samples are shown in Figure 4. It is seen that the morphology of the particles with the increase of praseodymium for content of x=0.4 and 0.6 is deviates from the spherical state and appears as a plate like. The non-uniformity in morphology and particle size is especially evident in Figure 4-c. The larger particles seems to be related to the Pr-Fe oxide phase, which appears mainly in the form of plates with the thickness about less than 30 nm and diameter approximately more than 100 nm. EDS analysis of samples and the weight percent of the elements are presented in Figure 5 and Table 4, respectively. It is

TABLE 3. Lattice parameter of the synthesized NPs with different concentrations of Pr value

Sample	Pr0	Pr2		Pr4		Pr6	
		Zn- Co Ferrite	Pr –Fe Oxide	Zn- Co Ferrite	Pr –Fe Oxide	Zn- Co Ferrite	Pr –Fe Oxide
$2\Theta_1$ (°)	35.37	35.48	32.53	35.48	32.56	35.78	32.68
$2\Theta_2$ (°)	62.46	30.15	46.66	62.69	46.68	30.23	46.81
$2\Theta_3$ (°)	56.88	62.67	58.23	30.22	58.27	62.90	58.34
d_1 (Å)	2.54	2.53	2.75	2.53	2.75	2.51	2.74
d_2 (Å)	1.49	2.96	1.95	1.48	1.94	2.95	1.94
d_3 (Å)	1.62	1.48	1.59	2.96	1.59	1.48	1.58
a (Å)	8.4	8.38	6.47	8.39	6.48	8.35	6.47

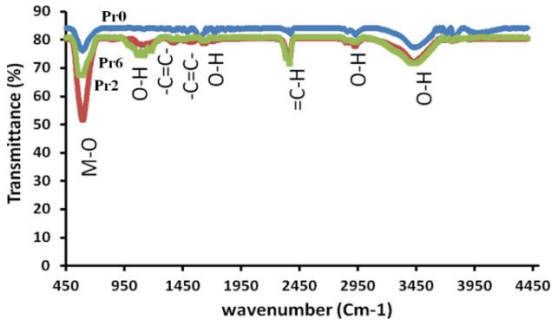

Figure 3. FTIR spectra of the synthesized samples as a function of Pr value

natural that by substituting Pr instead of iron in the composition and increasing its concentration, the presence of this element also increases and the concentration of Fe decreases. The concentrations of other elements (Co, Zn, O) are also changed by maintaining their atomic ratio in the composition. The extracted data are close to the stoichiometric state of the desired compounds.

Magnetic properties of the synthesized samples were investigated using VSM analysis (Figure 6) and the results are given in Table 5.

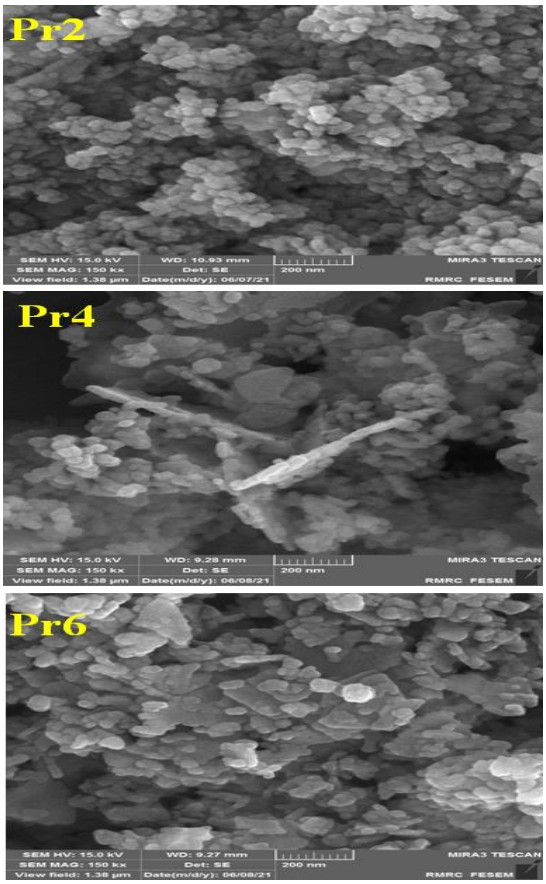

Figure 4. FESEM images of the synthesized samples with different Pr values

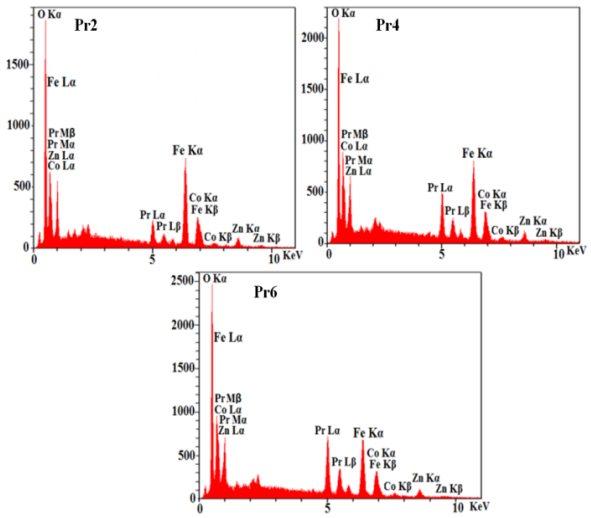

Figure 5. EDS analysis of NPs with different concentration of Pr element

The composition without the element praseodymium (cobalt-zinc ferrite; Pr0) has excellent magnetic properties, so that its saturation magnetization and coercive force at 10^4 Oe are 100.34 emu/g and 150 Oe,

TABLE 4. Weight percent of elements in synthesized samples containing various praseodymium

Sample	O	Fe	Co	Zn	Pr
Pr2	32.30	31.09	13.47	8.81	14.32
Pr4	29.07	24.78	12.39	8.04	25.72
Pr6	29.64	18.73	10.88	7.58	33.16

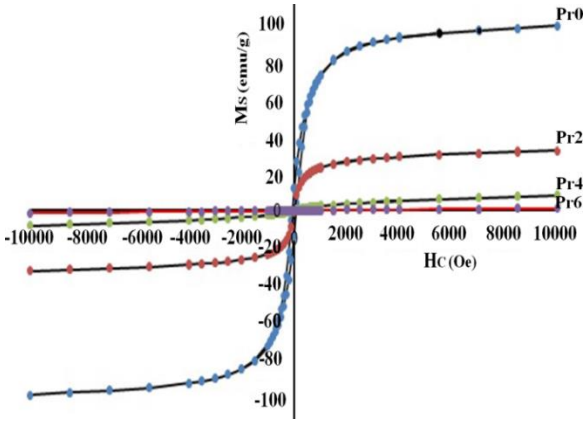

Figure 6. Magnetic hysteresis loops of the synthesized NPs as a function of Pr value

TABLE 5. Magnetic properties obtained from the hysteresis loops in terms of different concentrations of the Pr element

Magnetic properties	Pr0	Pr2	Pr4	Pr6
M (emu/g) at (3000 Oe)	91.54	28.22	4.58	0.43
M (emu/g) at (4000 Oe)	94.16	29.26	5.31	0.56
M (emu/g) at (5500 Oe)	96.48	30.37	6.23	0.76
M (emu/g) at (7000 Oe)	98.01	31.32	6.99	0.94
M (emu/g) at (8500 Oe)	99.18	32.03	7.67	1.12
Ms (emu/g) at (10000 Oe)	100.34	32.72	8.34	1.31
Hc (Oe)	150	~ 0	~ 0	~ 0
Mr (emu/g)	12.16	0.07	0.03	0.01
Mr /Ms	0.121	0.002	0.004	0.008

respectively. By adding the element Pr to the composition, the magnetic properties are drastically reduced and the sample becomes a completely non-magnetic material. The question is, what is the reason for these drastic changes? It should be noted that if the powders were a single phase (as in the Pr0 sample), since this phase (ZnCo ferrite) is a magnetic material, changes in magnetic properties could be attributed to changes in microstructure such as crystallite diameter and particle size. In this case, due to the decrease in crystallite diameter (Table 2) and particle size (Figure 4), it was expected that the Ms would decrease and the Hc would

increase. However, we see here that the coercive forces are completely eliminated and are almost zero, and the saturation magnetization of the samples are very negligible, especially for composition containing Pr equal to x=0.6 (1.31 emu/g). Therefore, it is concluded that this change is due to the magnetic nature of the powder and its conversion to a non-magnetic material with the formation of $PrFeO_3$ phase, and not the microstructure. However, the microstructure of the samples, as shown in Figure 4, had non-uniform particles containing ZnCo ferrites and Pr-Fe oxides which made effect on the magnetic properties.

4. CONCLUSIONS

Contrary to the initial predictions of solid solution formation with the entry of the element praseodymium into the crystal lattice, in the present study this does not happen at least for Pr values higher than x=0.2 and a secondary phase of $PrFeO_3$ forms next to the primary ZnCo ferrite phase. By increasing the presence of Pr in the composition, especially at x=0.6, about 84% by weight of the $PrFeO_3$ phase is formed and a completely non-magnetic material with zero coercive force and almost negligible saturation magnetization (1.13 emu/g) is produced. It has no positive effect on improving magnetic properties. However, the formation of plate like particles with the thickness about less than 30 nm can be seen in the sample containing Pr with x=0.6. Due to the magnetic properties of the Pr-doped sample with x= 0.2, it seems that if smaller amounts of this additive are used in the initial compositions, it is possible to create a solid solution of the initial ferrite and improve the microstructure because of particle size control.

5. ACKNOWLEDGEMENTS

The authors would like to acknowledge Department of Materials Engineering, Babol Noshirvani University of Technology.

6. REFERENCES

1. Manohar, A., Krishnamoorthi, C., "Synthesis and magnetic hyperthermia studies on high susceptible $Fe_{1-x}Mg_xFe_2O_4$ superparamagnetic nanospheres", ***Journal of Magnetism and Magnetic Materials*** 443, (2017), 267-274. DOI: 10.1016/j.jmmm.2017.07.065

2. Puspitasari, P., Budi, L.S., "Physical and magnetic properties comparison of cobalt ferrite nanopowders using sol-gel and sonochemical methods", ***International Journal of Engineering, Transactions B: Applications,*** Vol. 33, No. 5, (2020), 877-884. DOI:10.5829/ije.2020.33.05b.20

3. Linh, P.H., Anh, N.T.N., Nam, P.H., Bach, T.N., Lam, V.D., Manh, D.H., "A Facile Ultrasound Assisted Synthesis of Dextran-Stabilized $Co_{0.2}Fe_{0.8}Fe_2O_4$ Nanoparticles for Hyperthermia Application", ***IEEE Transactions on Magnetics*** 54, No. 6, (2018), 1-4. DOI: 10.1109/TMAG.2018.2815080

4. Nekouee, Kh.A., Rahimi, A.H., Alineghad, M., Ehsani, N., "The effect of Bismuth oxide on microstructures and magnetic properties of Mn-Mg-Al ferrites", ***Journal of Electronic Materials*** 47, No. 7, (2018), 4078-4084. DOI: 10.1007/s11664-018-6297-3

5. Yazdani, B., Nikzad, L., Vaezi, M.R., "Synthesis of $CoFe_2O_4$-polyaniline nanocomposite and evaluation it's magnetic properties", ***International Journal of Engineering, Transactions B: Applications,*** Vol. 22, No. 4, (2009), 381-386.

6. Topkaya, R., Baykal, A., Demir, A., "Yafet–Kittel-type magnetic order in Zn-substituted cobalt ferrite nanoparticles with uniaxial anisotropy", ***Journal of Nanoparticle Research*** 15, No. 1, (2013), 1954-1962. DOI 10.1007/s11051-012-1359-6

7. Dalal, M., Das, A., Das, D., Ningthoujam, R.S., Chakrabarti, P.K., "Studies of magnetic, Mössbauer spectroscopy, microwave absorption and hyperthermia behaviour of Ni-Zn-Co-ferrite nanoparticles encapsulated in multi-walled carbon nanotubes", ***Journal of Magnetism and Magnetic Materials,*** (2018). DOI: 10.1016/j.jmmm.2018.03.048

8. Ramakrishna, A., Murali, N., Margarette, S.J., Mammo, T.W., Joythi, N., Sailaja, B., Kumari, C.C., Samatha, K., Veeraiah, V., "Studies on structural, magnetic, and DC electrical resistivity properties of $Co_{0.5}M_{0.37}Cu_{0.13}Fe_2O_4$ (M = Ni, Zn and Mg) ferrite nanoparticle systems", ***Advanced Powder Technology*** 29, (2018), 2601-2607. DOI: 10.1016/j.apt.2018.07.005

9. Naik, S.R., Salker, A.V., "Change in the magneto structural properties of rare earth doped cobalt ferrites relative to the magnetic anisotropy", ***Journal of Materials Chemistry*** 22, (2012), 2740-2750. DOI: 10.1039/C2JM15228B

10. Xavier, S., Thankachan, S., Jacob, B., Mohammed, E., "Effect of Samarium Substitution on the Structural and Magnetic Properties of Nanocrystalline Cobalt Ferrite", ***Journal of Nanoscience,*** (2013), 1-7. DOI: 10.1155/2013/524380

11. Alves, T., Pessoni, H., Franco, A., "The effect of Y^{3+} substitution on the structural, optical band-gap, and magnetic properties of cobalt ferrite nanoparticles", ***Physical Chemistry Chemical Physics,*** (2017), 1-12. DOI: 10.1039/C7CP02167D

12. Panda, R.N., Shih, L.C., Chin, T.S., "Magnetic properties of nano-crystalline Gd-or Pr-substituted $CoFe_2O_4$ synthesized by the citrate precursor technique", ***Journal of Magnetism and Magnetic Materials*** 257, (2003), 79-86. DOI: 10.1016/S0304-8853(02)01036-3

13. Shahbahrami, B., Rabiee, S.M., Shidpoor, R., "An Overview of Cobalt Ferrite Core-Shell Nanoparticles for Magnetic Hyperthermia Applications", ***Advanced Ceramics Progress*** 6, (2020), 1-15. DOI: 10.30501/acp.2020.105923

14. Deatsch, A.E., Evans, B.A., "Heating efficiency in magnetic nanoparticle hyperthermia", ***Journal of Magnetism and Magnetic Materials*** 354, (2014), 163-172. DOI:10.1016/j.jmmm.2013.11

15. Mallick, A., Mahapatra, A.S., Mitra, A., Greneche, J.M., Ningthoujam, R.S., Chakrabarti, P.K., "Magnetic properties and bio-medical applications in hyperthermia of lithium zinc ferrite nanoparticles integrated with reduced graphene oxide", ***Journal of Applied Physics,*** 123, No. 5, (2018), 1-9. DOI: 10.1063/1.5009823

16. Pachpinde, A.M., Langade, M.M., Lohar, K.S., Shirsath, S.E., "Impact of larger rare earth Pr^{3+} ions on the physical properties of chemically derived $Pr_xCoFe_{2-x}O_4$ nanoparticles", ***Chemical Physics*** 429, (2014), 20-26. DOI:10.1016/j.chemphys.2013.11.018

17. Mahdikhah, V., Ataie, A., Babaei, A., Sheibani, S., Yang, C.W.O., Abkenar, S.K., "Control of structural and magnetic

characteristics of cobalt ferrite by post calcination mechanical milling", ***Journal of Physics and Chemistry of Solids*** 134, (2019) 286-294. DOI: 10.1016/j.jpcs.2019.06.018

18. Dhiwahar, A.T., Sundararajan, M., Sakthivel, P., Dash, C.S., Yuvaraj, S., "Microwave-assisted combustion synthesis of pure and zinc-doped copper ferrite nanoparticles: Structural, morphological, optical, vibrational, and magnetic behaviour", ***Journal of Physics and Chemistry of Solids*** 138, (2020), 109257. DOI: 10.1016/j.jpcs.2019.109257
19. Sinfroni, F.S.M., Santana, P.Y.C., Coelho, S.F.N., Silva, F.C., Menezes, A.S.D., Sharma, S.K., "Magnetic and structural properties of cobalt- and zinc-substituted nickel ferrite synthesized by microwave-assisted hydrothermal method", ***Journal of Electronic Materials*** 46, No. 2, (2017), 1145-1154. DOI: 10.1007/s11664-016-5081-5
20. Hanish, H.H., Edrees, S.J. Shukur, M.M., "The Effect of Transition Metals Incorporation on the Structural and Magnetic Properties of Magnesium Oxide Nanoparticles", ***International Journal of Engineering, Transactions A: Basics,*** Vol. 33, No. 4, (2020), 647-656. DOI: 10.5829/ije.2020.33.04a.16
21. Cullity, B.D., Elements of X-ray Diffraction, Massachusetts: Addison-Wesley Publishing Company, 1978.
22. Pilati, V., Gomes, R.C., Gomide, G., Coppola, P., Silva, F.G., Paula, F.L.O., Perzynski, R., Goya, G.F., Aquino, R., Depeyrot, J., "Core/Shell Nanoparticles of Non-Stoichiometric Zn-Mn and Zn-Co Ferrites as thermo sensitive Heat Sources for Magnetic Fluid Hyperthermia", ***Journal of Physical Chemistry C*** 122, No. 5, (2018), 3028-3038. DOI:10.1021/acs.jpcc.7b11014.
23. Asogekar, P.A., Verenkar, V.M.S., "Structural and magnetic properties of nanosized $Co_xZn_{(1-x)}Fe_2O_4$ (x= 0.0, 0.5, 1.0) synthesized via autocatalytic thermal decomposition of hydrazinated cobalt zinc ferrous succinate", ***Ceramics International*** 45, (2019), 21793-21803. DOI: 10.1016/j.ceramint.2019.07.182
24. Moravvej-Farshi, F., Amishi, M., Nekouee, Kh.A., "Influence of different milling time on synthesized Ni-Zn ferrite properties by mechanical alloying method", ***Journal of Materials Science: materials in Electronics*** 31, (2020), 13610-13619. DOI: 10.1007/s10854-020-03917-3
25. Moslehi-Niasar, M., Molaei, M.J., Aghaei, A., "Electromagnetic Wave Absorption Properties of Barium Ferrite/Reduced Graphene Oxide Nanocomposites", ***International Journal of Engineering, Transactions C: Aspects,*** Vol. 34, No. 6, (2021) 1505-1513. DOI: 10.5829/ije.2021.34.06c.14

Persian Abstract

چکیده

به منظور بررسی اثر Pr بر ریزساختار و خواص مغناطیسی ترکیب فریت کبالت–روی، مقادیر مختلف از Pr (x معادل ۰/۲، ۰/۴ و ۰/۶) با استفاده از مواد اولیه نیتراتی و به روش هم‌رسوبی به ترکیب اولیه ($Co_{0.6}Zn_{0.4}Fe_{2-x}Pr_xO_4$) افزوده شد. رسوبات حاصل در دمای ۷۵۰ °C به مدت ۲ ساعت کلسینه شدند. نمونه‌های سنتز شده با آنالیزهای الگوی پراش اشعه ایکس (XRD)، میکروسکپ الکترونی نشر میدانی (FESEM)، طیف‌نگاری فوریه (FTIR) و مگنتومتر نمونه ارتعاشی (VSM) مشخصه‌یابی شدند. بررسی XRD نشان داد که با افزودن Pr به ترکیب $Co_{0.6}Zn_{0.4}Fe_2O_4$ علاوه بر فاز فریت کبالت- روی، فاز ثانویه اکسید آهن--پرازئودمیم نیز تشکیل می‌شود. تصاویر میکروگراف پودرهای سنتز شده تغییراتی را در شکل و اندازه ذرات سنتز شده با افزودن Pr به ترکیب نشان دادند. برای نمونه با x=۰/۲، ذرات کروی شکل یکنواختی با اندازه حدوداً کمتر از ۶۰ nm تشکیل شدند. در حالیکه، برای ترکیب با x=۰/۶، پودری غیریکنواخت با ذرات صفحه‌ای شکل بدست آمد و نانو ذرات ضخامتی کمتر از ۳۰ nm داشتند. آنالیز مگنتومتر نمونه ارتعاشی (VSM) حکایت از تغییر خواص مغناطیسی قابل توجه فریت کبالت- روی به یک ماده کاملاً غیر مغناطیس با افزودن پرازئودمیم به ویژه برای مقادیر بالاتر از x=۰/۲ دارد.